View metadata, citation and similar papers at core.ac.uk

brought to you by CORE

provided by Queensland University of Technology ePrints Archive

QUT Digital Repository:
http://eprints.qut.edu.au/

This is the author version published as:

Little, Judith Paige and Pearcy, Mark J. and Tevelen, Gregory and Evans, John H. and Pettet, Graeme J. and Adam, Clayton J. (2010) ***The mechanical response of the ovine lumbar anulus fibrosus to uniaxial, biaxial and shear loads***. Journal of the Mechanical Behavior of Biomedical Materials, 3(2). pp. 146-157.

Copyright 2010 Elsevier

TITLE:

The mechanical response of the ovine lumbar anulus fibrosus to uniaxial, biaxial and shear loads

AUTHORS:

J P Little[1,3], M J Pearcy[1,3], G Tevelen[3], J H Evans[1,3], G Pettet[2,3], C J Adam[1,3]

AFFILIATION:

[1] School of Engineering Systems, Queensland University of Technology, Brisbane, Australia

[2] School of Mathematical Science, Queensland University of Technology, Brisbane, Australia

[3] Institute of Health and Biomedical Innovation, Queensland University of Technology, Brisbane, Australia

CORRESPONDING AUTHOR:

Dr J Paige Little

BEE Research Portfolio

O Block – Level 7

Gardens Point Campus

2 George Street

Brisbane QLD 4000

AUSTRALIA

Ph: +61 7 3138 5112

Email: j2.little@qut.edu.au

KEYWORDS

lumbar spine, intervertebral disc, anulus fibrosus, stiffness, mechanical testing, uniaxial compression, biaxial compression, simple shear

ABSTRACT

Analytical and computational models of the intervertebral disc (IVD) are commonly employed to enhance understanding of the biomechanics of the human spine and spinal motion segments. The accuracy of these models in predicting physiological behaviour of the spine is is intrinsically reliant on the accuracy of the material constitutive representations employed to represent the spinal tissues. There is a paucity of detailed mechanical data describing the material response of the *reinforced-ground* matrix in the anulus fibrosus of the IVD. In the present study, the 'reinforced-ground matrix' was defined as the matrix with the collagen fibres embedded but not actively bearing axial load, thus incorporating the contribution of the fibre-fibre and fibre-matrix interactions. To determine mechanical parameters for the anulus ground matrix, mechanical tests were carried out on specimens of ovine anulus, under unconfined uniaxial compression, simple shear and biaxial compression.

Test specimens of ovine anulus fibrosus were obtained with an adjacent layer of vertebral bone/cartilage on the superior and inferior specimen surface. Specimen geometry was such that there were no continuous collagen fibres coupling the two endplates. Samples were subdivided according to disc region - anterior, lateral and posterior - to determine the regional inhomogeneity in the anulus mechanical response. Specimens were loaded at a strain rate sufficient to avoid fluid outflow from the tissue and typical stress-strain responses under the initial load application and under repeated loading were determined for each of the three loading types.

The response of the anulus tissue to the initial and repeated load cycles was significantly different for all load types, except biaxial compression in the anterior anulus. Since the maximum applied strain exceeded the damage strain for the tissue, experimental results for repeated loading reflected the mechanical ability of the tissue to carry load, subsequent to the initiation of damage.

To our knowledge, this is the first study to provide experimental data describing the response

of the ‘reinforced-ground matrix’ to biaxial compression. Additionally, it is novel in defining a study objective to determine the regionally inhomogeneous response of the ‘reinforced-ground matrix’ under an extensive range of loading conditions suitable for mechanical characterisation of the tissue. The results presented facilitate the development of more detailed and comprehensive constitutive descriptions for the large strain nonlinear elastic or hyperelastic response of the anulus ground matrix.

1. INTRODUCTION

The intervertebral disc is a complex load-bearing structure in the spine, which when healthy, consists of a gel-like hydrostatic *nucleus pulposus* (Nachemson 1960), surrounded circumferentially by layers (lamellae) of anulus ground matrix reinforced with collagen fibres (Akeson *et al.* 1977), the *annulus fibrosus*. During physiological loading, the intervertebral disc (IVD) components are subjected to a complex combination of load states (Klein and Hukins 1983). Pressurization of the nucleus pulposus generates circumferential hoop stress in the anulus fibrosus, thus tensioning the anulus collagen fibres, while axial loading of the spinal column by gravitational and muscle forces, results in compression of the anulus ground matrix (Akeson *et al.* 1977).

The anulus fibrosus consists predominantly of type I collagen fibres embedded within a ground matrix comprised of water, proteoglycans and non-collagenous proteins. The collagen fibres are oriented obliquely to the transverse plane of the disc within the anulus lamellae. Additionally, elastin fibres exist between the lamellae and ‘bridge’ across the lamellae (Yu *et al.* 2002). The mechanical response of the anulus fibrosus is governed by the structural contributions from both the anulus ground matrix (which due to its proteoglycan rich biochemistry is well suited to resisting compression and tension), and the collagen fibres, which resist tensile load states. Additionally, the mechanical (frictional) interaction between the collagen fibres and the ground matrix and cross-linking between fibre bundles within the matrix, play a role in governing the mechanical behaviour of the anulus fibrosus (Adams and Green 1993; Pezowicz *et al.* 2006; Schollum *et al.* 2008; Wagner and Lotz 2004).

Analytical and computational models are commonly used to investigate the mechanics of the healthy and diseased spine (Little *et al.* 2007; Rohlmann *et al.* 2006; Shirazi-Adl *et al.* 1986; Zander *et al.* 2001). The accuracy of these models in simulating physiological behaviour is intrinsically reliant upon the accuracy of the material constitutive representations employed for the structures modelled. When studying the biomechanics of a single motion segment, the IVD’s play a crucial role in defining the kinematics and kinetics of the joint (Adams *et al.* 1980). Finite Element

(FE) models of the anulus fibrosus commonly represent the IVD as a fibre-reinforced composite, using either linear or nonlinear elastic (hyperelastic) constitutive laws with tension-only reinforcing members simulating the collagen fibres (Little *et al.* 2007; Rohlmann *et al.* 2006; Shirazi-Adl *et al.* 1986; Zander *et al.* 2001).

Extensive experimental data to accurately quantify parameters for constitutive models of the anulus fibrosus are not readily available in the literature. . In particular, there is a paucity of data which could allow the mechanical properties of the 'reinforced-ground matrix'♦, in isolation of the tension-only stiffness contribution of the collagen fibres, to be determined. While many previous studies have investigated the response of the anulus fibrosus to uniaxial (compressive, tensile or shear) loading (Acaroglu *et al.* 1995; Best *et al.* 1994; Iatridis *et al.* 1999, 2005; Kasra *et al.* 2004; Skaggs *et al.* 1994a) these data are seldom applicable for the derivation of material constants relating to the reinforced-ground matrix. Moreover, we are aware of only one existing investigation of the biaxial response of the anulus fibrosus (Bass *et al.* 2004), however this was carried out for tensile loading. Arguably, the anulus ground matrix experiences predominantly compressive load states during physiological activities (as opposed to the embedded collagen fibres which resist tension). Bass *et al* (2004) note that data for the 'complete three dimensional stress and strain field' are imperative for the definition of a constitutive law governing a tissues mechanical behaviour.

The P-Q curve, as used in classical continuum mechanics, provides a useful method of representing the combination of hydrostatic pressure (P) and pure deviatoric shear (Q) stress to which a structure is subjected under any given loading state (Figure 1). This curve demonstrates that a comprehensive 'map' of the mechanical behaviour of a material can be obtained by quantifying the response of the material to varied loading conditions. As such, performing uniaxial, biaxial and shear testing of a material provides useful mechanical constitutive data over a considerable region of the P-Q stress space.

The present study sought to provide a comprehensive envelope of data for the mechanical response of the reinforced-ground matrix in the ovine IVD anulus fibrosus, in a form suitable for computational simulations of the disc. Specifically, we assess the effect of loading type (uniaxial compression, biaxial compression and simple shear), anatomical location (between anterior, lateral and posterior anulus) and the effect of repeated loading on the ground matrix mechanical properties.

♦For the purposes of this study, the term 'reinforced-ground matrix' will refer to the mechanical function of the anulus ground matrix with fibres embedded within this matrix, but not actively bearing axial load. Thus this term encapsulates both the mechanical behaviour of the ground matrix as well as the influence of the fibre-fibre and fibre-matrix interactions on the tissue mechanics.

2. METHODS

In the present research, excised anulus fibrosus ground matrix specimens from three regions within the ovine lumbar IVD were loaded under uniaxial compression, biaxial compression and simple shear. In the case of uniaxial and biaxial testing of the ground matrix, compression loading was preferable to tensile loading, to avoid unnecessarily tensioning the residual collagen fibres in the specimens. Typical stress-strain responses under the initial load application and under repeated loadings were determined.

2.1. Rationale for experimental approach

There are three approaches which could be adopted to experimentally characterise the deformation response of fibre-reinforced IVD composite structure; the first is to measure the overall response of the composite material, without consideration of the individual constituents. However, this approach is most appropriate for simple loading states (e.g. uniaxial tension/compression/shear). The second approach is to characterise the mechanical properties for the fibres and for the 'reinforced-ground matrix' (i.e. the fibre plus matrix composite) separately. The third approach would involve extensive experimental characterisation of both the fibres (in axial and non-axial loading directions) and the ground matrix as well as specifically characterising the fibre-fibre and fibre-matrix mechanical interactions.

The second approach is an accepted modelling approach for fibre-reinforced composites commonly used in existing computational studies of the spine (Little et al. 2007; Rohlmann et al. 2006; Shirazi-Adl et al. 1986; Zander et al. 2001). As such, the experimental approach employed in the present study was to capture mechanical data for the reinforced-ground matrix.

2.2. Specimen Harvesting

Sheep discs have been shown to exhibit similar kinematic and biochemical properties to human discs (Reid *et al.* 2002; Wilke *et al.* 1997). Seven IVD's were sectioned from the frozen lumbar spines of six sheep - two L3/4, one L4/5 and four L6/7 discs were obtained. The posterior elements, spinal cord and surrounding musculature were removed. A 1-3mm layer of cartilaginous endplate and vertebral bone on the superior and inferior surfaces of the discs were preserved (Figure 3). While sectioning the discs from the spines they were kept moist with Ringers solution and the room temperature was maintained at 20^{o}c. Generally the disc had not thawed by the time it was isolated from the spine. The discs were then surrounded with Ringers soaked muslin,

sealed in air tight bags and refrozen to -20°c. Once frozen the individual discs were set in dental cement in preparation for sectioning into test specimens (Figure 2). A plasticine mold was used to shape the dental cement. The mold was frozen at -20°c and was placed in cold water, while the uncured cement was poured over the disc. These steps were carried out to create a heat sink for the exothermic curing of the dental cement. The dental cement plug with embedded disc was cured for 1 hour at room temperature, then frozen at -20°c for a further 20 hours.

To obtain mechanical data for the reinforced-anulus ground matrix rather than the ground matrix-collagen fibre composite, we ensured that no continuous collagen fibres coupled the two endplates of the specimens (Figure 3). This was achieved by calculating a specimen width to ensure fibres at an inclination of between 31° and 39° (range of collagen fibre inclination) (Marchand and Ahmed 1990) would not connect the endplates of the sheep discs. The disc heights ranged between 3-5mm. As such, the mechanical response of the specimens represented the bulk response of the ground matrix with the fibres embedded but not actively bearing a load.

A precision anular microsaw (Microslice 2, Malvern Instruments Ltd, Malvern, UK) with diamond tipped blade was employed to section test pieces from the intact disc embedded in dental cement (Figure 2). Cuts were made parallel to the sagittal and frontal planes through the disc (Figure 3 A), such that the full disc height and superior and inferior bone layers were preserved in the test specimens (Figure 3 B). The blade was advanced by 3mm after each successive cut in a plane (saw accuracy, 0.1mm). This produced test specimens with a square cross-section of 3×3 (± 0.2) mm (Figure 3 B). The disc tissue was kept moist during the cutting process.

Once sectioned from the disc, any test specimens that contained nucleus material were discarded. Curing of polymethymethacrylate is an exothermic reaction which has been shown to cause tissue necrosis (Lieu *et al.* 2001). To ensure damaged specimens weren't used for testing, anulus specimens from the peripheral disc were also discarded as these were in direct contact with the dental cement during curing. The mechanical response of the anulus fibrosus is region dependent (Acaroglu *et al.* 1995; Fujita *et al.* 1997; Skaggs *et al.* 1994b), therefore, samples were obtained from the anterior, lateral and posterior disc regions (Figure 3A). Anulus specimens were labelled according to disc region (anterior, lateral or posterior), wrapped in Ringers soaked muslin, sealed in clip seal bags and frozen to -20°C. Specimens were frozen for a maximum of 5 days before being tested.

The region-specific specimens from each disc were randomly assigned to one of three groups for uniaxial compression, biaxial compression and simple shear testing (Table 1). All specimen dimensions were measured before testing, and engineering stress and strain were calculated based on the original dimensions.

	Total Number of specimens	Anterior specimens	Lateral specimens	Posterior specimens
Uniaxial Compression	32	14	9	9
Simple Shear	23	10	8	8
Biaxial Compression	24	9 (5 radial, 4 circumferential)	8 (3 radial, 5 circumferential)	7 (3 radial, 4 circumferential)

Table 1. Specimen details

2.3. Biaxial Compression Testing

A novel testing rig was designed and built to carry out the biaxial compression testing (Figure 4). Complete details of the design methodology, commissioning and calibration of this rig are detailed elsewhere (Little *et al.* 2009). In brief, the device was a rectangular pressure vessel, with viewing windows on two of the four vertical sides to allow measurement of the specimen deformation using a Sigmascope 300 Shadowgraph profile projector (Herbert Controls and Instruments Ltd, Letchworth, UK, Accuracy=0.001mm). Attachment sites for the specimens were located on the intermediate vertical walls. The design objective for the rig was to apply a hydrostatic compressive pressure to the specimen, while simultaneously unloading the specimen along the long axis, thus creating a state of equibiaxial compression. The specimens were attached to the walls using inextensible nylon thread; one of the bone surfaces was rigidly attached while the other end of the specimen was attached to the end of a ceramic piston (Figure 4 B, C). This piston was freely floating on a thin layer of fluid in a highly polished cylindrical bore in the opposite wall, thus minimising frictional resistance. The vessel was filled with Ringer's solution, which was pressurised during testing using a Norgren precision pressure regulator (Model:11-818, IMI Norgren Ltd, Staffordshire, UK, Max Press: 408 kPa (60psi), Accuracy: 3 kPa (0.435psi)). Biaxial pressure in the vessel was measured during testing using a Druck pressure calibrator (DPI 705, GE Druck Ltd, Leicester UK) and specimen deformation measured using the Shadowgraph profile projector.

2.4. Uniaxial Compression Testing

Uniaxial compression of the anulus specimens was carried out on a single axis Hounsfield testing machine (Tinius Olsen Ltd, Surrey, UK). The upper and lower bone surfaces were glued to the loading platens, such that compressive loading on the specimen was oriented in the axial direction and there was no risk of specimen slip between the platens.

2.5. Simple Shear Testing

Pure shear (no hydrostatic stress) is a difficult stress state to achieve experimentally with small biological tissue samples, therefore, simple shear loading was carried out. Using relationships between pure shear strain energy density (U) and simple shear stress proposed by Treloar (1975), the equivalent pure shear state (stress and strain) associated with the applied simple shear was calculated (**Error! Reference source not found.**This required data for the maximum principal simple shear extension ratio, which were calculated from the simple shear data using a strain ellipsoid (Treloar 1975). (Extension ratio is defined as the ratio between the final deformed dimension and the undeformed dimension.)

Simple shear tests were carried out using purpose built test fixtures on the same single axis Hounsfield testing machine as described above (Figure 5). (Hounsfield loadcell force accuracy = 0.5% applied force; Hounsfield extension accuracy = 0.01 mm; specimen cross-sectional dimension accuracy = ± 0.02 mm). The bone surfaces on each specimen were glued to fixtures, A and B, which were attached to the load cell and to the machine crosshead, respectively. The distance between the fixtures A and B was controlled such that the specimen fit was flush between the fixtures, thus avoiding axial preload in the tissue. This was further ensured since the chain-link attachment between fixture A and the load cell ensured the specimen was not unintentionally preloaded. The simple shear load was oriented parallel to the lamellae in the specimen (ie. circumferentially in an intact disc). When the crosshead was driven downward during testing, this generated simple shear in the transverse plane of the specimen – the out-of-plane extension ratio (ie. radially in an intact disc) was zero and the extension ratio perpendicular to the load direction (ie. axially in an intact disc) was the reciprocal of the extension ratio in the load direction. As such, for simple shear loading to be achieved in the sample, the distance between the faces of fixtures A and B decreased during testing.

2.6. Testing Protocol

Ultimate failure strains for the anulus fibrosus under tensile loading are reported to range between 21.3 ± 2.1% (Iatridis *et al.* 2005) for circumferential loading to 56.8% ± 29.7% (Kasra *et al.* 2004) for axial loading. It has been previously established that the strain to initiate damage in the anulus ground substance ranged from 20-27% under uniaxial compression and from 20-30% under simple shear loading (Little 2004). During physiological loading, the ground matrix could conceivably be subjected to strains exceeding these values (Kasra *et al.* 1992; Little *et al.* 2007) . As such, specimens were loaded to a maximum strain that reflected the range of strains to which the anulus ground substance is subjected physiologically. Since this maximum strain exceeded the damage strain for the tissue, experimental results for repeated loading reflected the mechanical ability of the tissue to carry load, subsequent to the initiation of damage.

The data on the ground matrix response to both initial and repeated load application were collected for each specimen. Under biaxial compression, a single specimen was loaded a total of seven times to a maximum stress of 0.2-0.25 MPa under load control. Specimens were permitted to recover for 15 minutes between each test and lateral deformation of the specimen (off-axis from the unloaded direction) was measured either in the plane of the lamellae (circumferentially in the unsectioned disc) or perpendicular to the lamellae (radially in the unsectioned disc). Of the 24 samples tested biaxially, 13 were oriented to measure circumferential deformation (Table 1). Specimens tested biaxially were preconditioned for five cycles to 5% strain at 1.5Hz.

A similar loading protocol was employed in determining the specimen response to uniaxial compression and simple shear. Each specimen was loaded five times to a maximum strain of 55-60% and the specimens were permitted to relax for five minutes between each load application. Specimens were kept hydrated during and between initial and repeated load applications for both uniaxial compression and simple shear using Ringer's soaked muslin and by surrounding them with a plastic sheet. Prior to both uniaxial compression and simple shear, the specimens were preconditioned for five cycles at 0.4Hz.

2.7. Strain Rate

A key study aim was to obtain experimental data representative of the tissue response to physiological loading rates. As such, the strain rate was selected in order to inhibit pore fluid flow/loss or volume change in the material. This was in keeping with the findings of Higginson *et al.* (1976). The majority of existing studies have investigated the response of the anulus at strain rates intended to minimise fluid drag through the pore spaces and promote fluid movement (Acaroglu *et al.* 1995; Best *et al.* 1994; Ebara *et al.* 1996; Fujita *et al.* 1997; Skaggs *et al.* 1994a; Wu and Yao 1976). Such studies used strain rates ranging from $0.00009sec^{-1}$ to $0.005sec^{-1}$ and were not intending to simulate the physiological loading condition. Morgan (1960) noted that the rupture strain of collagenous tissue is dependent on the strain rate at which it is loaded. Kasra *et al.* (2004) loaded region-specific samples of sheep anulus fibrosus in tension and noted that as the strain rate increased, the ultimate strain decreased. These authors used a strain rate of 0.014-$0.033sec^{-1}$ to represent a 'medium' as opposed to a 'slow' or 'fast' loading rate. In the present study, a strain rate of $0.01sec^{-1}$ was used.

While it has been shown that freezing of IVD specimens for extended periods of time may alter the creep response of the tissue (Bass *et al.* 1997), when loaded at higher strain rates as was the case in the present study, previous researchers have shown that freezing has a negligible effect on the observed mechanical response of the disc (Callaghan and McGill 1995; Panjabi *et al.* 1985).

2.8. Data Analysis

Raw data for each loading type was analysed using SPSS 11.0 (SPSS Australiasia Pty Ltd, Chicago, USA), to determine curves of best fit for the initial and repeated loading in each disc region (Curve types are shown in Figures 6 - 8). If there was no difference between the initial and repeat load response, all experimental curves for that specimen were used to determine the regression line for the repeated loading. The R^2 correlation co-efficient and the standard error of estimate was calculated for regression lines fit to each region. Analysis-of-Variance (ANOVA) was carried out to compare the initial and repeated regression curves in each disc region, to determine if they were significantly different from each other and between regions.

3. RESULTS

3.1 Uniaxial Compression

Characteristic specimen responses to uniaxial compression (Figure 6A) demonstrated a notably stiffer response to the initial load application (cycle 1) compared to subsequent loading (cycles 2-5). Repeated loading generally showed a compliant response up to a strain of 20-40% followed by a considerable increase in stiffness compared to the initial load application. The response to repeated loading was generally highly reproducible between successive cycles (Figure 6B). At higher uniaxial compressive strains, separation of the anulus lamellae was observed in less than 10% of the specimens (Shown schematically in Figure 6C). These separations were thought to be the cause of local drops in stiffness observed in the stress-strain response of these specimens. However, since this was not a consistently observed response for all specimens, the typical experimental responses shown in Figure 6 do not demonstrate these localised stiffness changes.

Comparison of the regression lines for the three anulus regions showed the posterior anulus was stiffest and the lateral was the most compliant for both the initial and repeated uniaxial loading (Figure 6D). The stress-strain response of the ground matrix was nonlinear, both for the initial and repeated loading cycles, however, repeated loading demonstrated a greater relative increase in stiffness over the strain range tested. ANOVA indicated there was a significant difference between the initial and repeated loading cycles for all anulus regions ($p < 0.001$).

3.2. Simple Shear

Results for simple shear testing demonstrated a similar characteristic to the tissue response under uniaxial compression – the specimen was more compliant upon repeated loading (cycles 2-5) in comparison to the initial load cycle (Figure 7 A). The response for cycles 2-5 was highly

repeatable. During simple shear loading the ground matrix demonstrated minimal bulge, with only slight swelling observed in the direction of the applied shear load (ie. circumferentially in the intact disc). After removal of the sample from the fixtures, following repeated shear loading, the sample was noticeably more lax.

Regression analysis to determine best fit curves for the three anular regions (Figure 7 B), under both initial and repeated loading cycles, showed the anterior anulus was the stiffest region and the posterior the most compliant. The response to cycles 2-5 was more compliant than for the initial loading cycle, at strains below 50%. ANOVA indicated there was a significant difference between the region specific tissue response for both the first and subsequent (2^{nd} to 5^{th}) loading cycles ($p<0.005$).

3.3. Biaxial Compression

The response to biaxial compression was dependent on the orientation of the specimen. Of the 13 specimens measured in the circumferential direction, 10 showed a stiffer response initially and a drop in stiffness for the repeated loading cycles (Figure 8 A). In two of these 10 specimens, this drop in stiffness was most obvious at low strains. There was no appreciable stiffness variation observed between the initial and repeated loading cycles in six of the nine specimens measured radially (Figure 8 B), while for the remaining three, there was a drop in stiffness apparent at low strains (Figure 8 C).

Regression lines for the biaxial compression data (Figure 8 D,E) showed the anterior anulus was the stiffest and the lateral anulus the most compliant during initial and repeated (2^{nd} to 7^{th}) loading cycles, when strain was measured radially. When deformation was measured circumferentially the posterior anulus was the stiffest and the anterior anulus the most compliant following initial and repeated loading cycles. ANOVA indicated there was no significant difference between the initial (first cycle) and repeated (2^{nd} to 7^{th} cycles) tissue response when strain was measured radially in the anterior anulus, so only one regression line was presented for these loading data. For all other anulus regions, there was a significant difference between the initial and repeated load cycle response ($p<0.001$). There was a significant difference between the radial and circumferential measurements when compared within a region, for the first load cycle ($p <= 0.001$) and repeated load cycles ($p < 0.005$).

4. DISCUSSION

In order to comprehensively assess the mechanical behaviour of the ovine lumbar anulus ground matrix, disc specimens were tested in uniaxial compression, simple shear and biaxial compression. Specimens were excised with careful consideration of the fibrous connection

between adjacent vertebral endplates, to ensure there was no continuous collagen fibre link, thus providing constitutive data on the ground matrix response, with embedded but non-axial load-bearing collagen fibres.

While the specimen dimensions were calculated to ensure the residual collagen fibres were not constrained by the adjacent vertebral endplates and therefore, would not actively carry load, these fibres still provided some resistance to the applied strain due to their frictional relationship with the surrounding matrix and their fibre-fibre interactions. However, this was considered a desirable artefact in the stress-strain response of the specimens. If the mechanical response of the ground substance alone was determined, then an analytical model of the anulus fibrosus would require data to quantify the relationship between the ground substance and the embedded fibres. Thus far, previous studies in this area have addressed the question of mechanically characterising the ground matrix interactions primarily for uniaxial tensile loading (Adams and Green 1993; Pezowicz *et al.* 2006). However, in the present study, we present data useful for a constitutive model which incorporates these interactions, negating the need for experimental methods to quantify the relevant matrix interaction parameters. As such, data from this study will provide direct input into constitutive model representations for the reinforced-ground matrix, which may be used in conjunction with a fibre-reinforced composite approach to representing the anulus fibrosus (Wagner and Lotz 2004) in computational models of the IVD.

Few existing studies have investigated simple shear loading (Fujita *et al.* 2000) as opposed to torsional shear testing (Iatridis *et al.* 1999) and to our knowledge, no prior study has investigated the biaxial compression loading response of the anulus tissue. Generally, previous studies investigating the compressive behaviour of the anulus fibrosus have been carried out to determine the stress-relaxation response and biphasic properties of the tissue (Best *et al.* 1994; Iatridis *et al.* 1998) and thus are carried out at slower strain rates than those used in the present study. Despite these limitations, Table 2 gives a qualitative comparison of previous experimental data with our study, highlighting the disc regions which have been observed to demonstrate the highest and lowest stiffness (determined as an elastic modulus). Comparing these data with the results presented in the present study, it may be seen that anulus ground matrix specimens in the present study demonstrated similar inhomogeneity in tissue stiffness (Table 3).

Region	Anterior, initial	Anterior, repeated	Lateral, initial	Lateral, repeated	Posterior, initial	Posterior, repeated
A.						
Equation type	$\ln(\sigma) = B0 + B1(\ln(\varepsilon)) + B2(\ln(\varepsilon))^2$	$\ln(\sigma) = B0 + B1(\ln(\varepsilon)) + B2(\ln(\varepsilon))^2 + B3(\ln(\varepsilon))^3$	$\ln(\sigma) = B0+B1(\ln(\varepsilon))+ B2(\ln(\varepsilon))^2$	$\ln(\sigma) = B0 + B1(\ln(\varepsilon)) + B2(\ln(\varepsilon))^2 + B3(\ln(\varepsilon))^3$	$\ln(\sigma) = B0 + B1(\ln(\varepsilon)) + B2(\ln(\varepsilon))^2$	$\ln(\sigma) = B0 + B1(\ln(\varepsilon)) + B2(\ln(\varepsilon))^2 + B3(\ln(\varepsilon))^3$
Constants	$B0 = 2.27^{*}$; $B1 = 3.47^{*}$; $B2 = 0.338^{*}$	$B0 = 6.125^{*}$; $B1 = 12.92^{*}$; $B2 = 4.613^{*}$; $B3 = 0.540^{*}$	$B0 = 2.717^{*}$; $B1 = 4.496^{*}$; $B2 = 0.556^{*}$	$B0 = 4.693^{*}$; $B1 = 11.54^{*}$; $B2 = 3.902^{*}$; $B3 = 0.435^{*}$	$B0 = 2.773^{*}$; $B1 = 3.766^{*}$; $B2 = 0.377^{*}$	$B0 = 6.361^{*}$; $B1 = 11.83^{*}$; $B2 = 3.664^{*}$; $B3 = 0.376^{*}$
R^2	.887	.838	.901	.800	.866	.802
Standard error of estimate	.632	.935	.607	1.117	.697	1.085
B.						
Equation type	$\ln(\sigma) = -B0.(-\ln(\varepsilon))^{B1}$	$\ln(\sigma) = B0 + B1(\ln(\varepsilon)) + B2(\ln(\varepsilon))^2 + B3(\ln(\varepsilon))^3$	$\ln(\sigma) = -B0.(-\ln(\varepsilon))^{B2}$	$\sigma = \exp(B0 + B1.\varepsilon)$	$\sigma = B0 + B1.\varepsilon + B2.\varepsilon^2 + B3.\varepsilon^3$	$\ln(\sigma) = B0 + B1(\ln(\varepsilon)) + B2(\ln(\varepsilon))^2 + B3(\ln(\varepsilon))^3$
Constants	$B0 = 3.553^{*}$; $B1 = 0.504^{*}$	$B0 = -0.160$; $B1 = 5.201^{*}$; $B2 = 1.529^{*}$; $B3 = 0.164^{*}$	$B0 = 4.224^{*}$; $B1 = 0.340^{*}$	$B0 = -6.859^{*}$; $B1 = 5.802^{*}$	$B0 = 0.002^{*}$; $B1 = 0.0602$; $B2 = -0.015$; $B3 = 0.1156^{*}$	$B0 = -2.204^{*}$; $B2 = 4.520^{*}$; $B2 = 1.710^{*}$; $B3 = 0.219^{*}$
R^2	.590	.743	.427	.663	.995	.840
Standard error of estimate	.231	.906	.188	.894	.002	.474
C.						
Equation type	$\sigma = B0+B1.\varepsilon+B2.\varepsilon^2$	$\ln(\sigma) = B0 + B1(\ln(\varepsilon)) + B2(\ln(\varepsilon))^2$	$\ln(\sigma) = -B0.(-\ln(\varepsilon))^{B1}$	$\ln(\sigma) = B0 + B1(\ln(\varepsilon)) + B2(\ln(\varepsilon))^2$	$\sigma = B0+B1.\varepsilon+B2.\varepsilon^2$	$\sigma = B0 + B1.\varepsilon + B2.\varepsilon^2$
Constants	$B0 = -0.002$; $B1 = 0.402$; $B2 = 0.884$	$B0 = 2.607^{*}$; $B1 = 3.962^{*}$; $B2 = 0.252$, ($p < 0.05$)	$B1 = 1.151^{*}$; $B1 = 1.110^{*}$	$B0 = -2.20$; $B1 = -4.01$; $B2 = -2.99^{*}$;	$B0 = 0^{*}$; $B1 = 0.781$; $B2 = 5.014^{*}$	$B0 = 0$; $B1 = 0$; $B2 = 8.680$
R^2 – Circ'l	.710	.800	.636	0.580	0.100^{**}	$.100^{**}$
Standard error of estimate	.040	1.144	.212	5.386	.0911	.113
D.						
Equation type	N/A	$\sigma = B0+B1.\varepsilon+B2.\varepsilon^2$	$\ln(\sigma) = B0+B1(\ln(\varepsilon))+ B2(\ln(\varepsilon))^2$	$-\ln(\sigma) = \exp(B0 - B1.\ln(\varepsilon))$	$\ln(\sigma) = B0 + B1(\ln(\varepsilon)) + B2(\ln(\varepsilon))^2$	$\ln(\sigma) = B0 + B1(\ln(\varepsilon)) + B2(\ln(\varepsilon))^2$
Constants		$B0 = 0$; $B1 = 0.50^{*}$; $B2 = 7.00$;	$B0 = 0.627$; $B1 = 1.132$; $B2 = -0.131$	$B0 = -1.381^{*}$; $B1 = 1.138^{*}$	$B0 = 3.387$, ($p < 0.05$); $B1 = 3.222^{*}$; $B2 = 0.316$	$B0 = 1.232$; $B1 = 0.907$; $B2 = -0.388^{*}$
R^2 — Rad'l	N/A	.790	.879	.923	.834	.965
Standard error of estimate		.042	.311	.259	.379	.475

*Equation constants have a $p < 0.01$ for a t-distribution.
**The low R^2 value reflects large variability observed in the biaxial data from these regions.

Table 2. Regression equations, equation constants, R^2 values and standard error of estimate for the initial and repeated loading response in the three disc regions for A uniaxial compression results; B. simple shear results; C. biaxial compression – circumferential; D. biaxial compression – radial (Note: the anterior initial and continued response are the same when measured radially).

Mechanical Testing	Source of data	"Highest stiffness" Region of Anulus	"Lowest stiffness" Region of Anulus
Uniaxial, unconfined compression	*Present Study*	*Posterior*	*Lateral*
Confined compression	Best *et al*. (1994) - creep test with study results analysed using biphasic theory	No significant diff. in aggregate modulus, (H_A, meas. of the mechanical response of the anulus fibrosus solid phase) betw the ant. & post. anulus. Although, the mean H_A in the post. anulus was higher than the mean ant. H_A.	
Simple Shear	Present study	Anterior	Posterior
	Fujita *et al*. (2000) - simple shear (circumferentially, radially and axially aligned)	Anterior	Posterior
Biaxial Compression	Present study – circum'l measurement	Posterior	Anterior
	Present study - radial measurement	Anterior	Lateral
Tensile	Acaroglu *et al*.(1995) (circum'l tension); Ebara *et al*.(1996) (circum'l tension)	Anterior	Posterolateral
	Smith *et al*.(2008) (radial tension)	Anterolateral	Posterolateral
	Fujita *et al.* (1997)	No siginificant difference between anterior and posterolateral tangent modulii	

Table 3. Comparison of experimental findings from the present study with data from previous researchers

Moreover, if a linear shear modulus is calculated up to 10% strain using the data from Figure 7B, the anterior and posterior shear moduli are 0.045MPa and 0.019MPa, respectively. These are the same order of magnitude as those presented by Fujita *et al.* (2000) (0.029 MPa and 0.022 MPa, respectively) for the G_{12} modulus of cadaveric anulus fibrosus. Similarly, if a linear elastic modulus is approximated up to 30% strain (the range tested by (Iatridis *et al.* 1998), using the data from Figure 6C, the resulting elastic modulus of 0.814MPa is in reasonable agreement with the aggregate modulus of 0.67MPa for cadaveric anulus fibrosus, which may be calculated using the experimental data presented by Iatridis *et al.* (1998).

Iatridis et al. (2005) observed a reduction in peak stress following quasi-static tensile loading of bovine annulus fibrosus to increasing proportions of the reported ultimate tensile strain (21.3 ± 2.1%). The reductions in peak strain were observed in some cases after the first load cycle. Similarly, in the present study, when loaded to strains in excess of the damage initiation strain, the ground substance showed a significant drop in stiffness upon repeated loading. Possibly, such a considerable reduction in stiffness would not occur in situ, in the presence of biological entities capable of initiating immediate tissue repair (Iatridis et al. 2005). Iatridis et al. (2005) noted that interlaminar separations were likely to be the most prominent cause for mechanical weakening of the anulus fibrosus specimens. Similarly, in the present study, the observed interlaminar separations were thought to be a possible cause for the loss of stiffness between the initial and repeated loading and possibly related to the considerable increase in laxity of the samples tested in simple shear.

Upon repeated loading, despite a significant reduction in tissue stiffness, the ground substance is still capable of resisting applied load, but with a notably different mechanical behaviour. Under uniaxial compression and simple shear, the repeated loading response may be subdivided into two regions – Region 1 demonstrates high compliance at low strains (strains less than 40%) and Region 2 demonstrates increased stiffness at higher strains. Moreover, the stiffness in Region 2 generally exceeds the stiffness observed during the initial load cycle. Overall, the repeated loading response is analogous to the mechanical response of the spinal motion segment; demonstrating a behaviour similar to a neutral zone. Thompson *et al.* (2003) observed an average increase of 50% in the neutral zone range of motion for sheep spinal motion segments when joints were subjected to repeated flexion loading before and after removal of the posterior elements and soft tissues – increasing from 3.9^{o} in the intact segment to 5.7^{o} in the 'disc only' segment. Iatridis *et al.* (2005) suggested some permanent damage may occur subsequent to tensile loading to strains below catastrophic strain, resulting in an increased laxity in the anulus tissue and an increased neutral zone. Similarly, results in the present study suggest there may be a similar increase in anulus ground substance laxity following loading to strains necessary to initiate tissue damage.

5. CONCLUSION

To the best of our knowledge, this study provides the first constitutive data on the uniaxial, biaxial and shear response of the reinforced- ovine lumbar anulus ground matrix. By quantifying the nonlinear stiffness and damage response of IVD ground matrix tissue, the results presented facilitate the development of more detailed and comprehensive constitutive descriptions for the large strain nonlinear elastic or hyperelastic response of the tissue. These constitutive laws are a necessary input to computational models of the lumbar spine, to provide more realistic biomechanical representations of spinal mechanics in health and disease.

6. FIGURE CAPTIONS

Figure 1. P-Q curve defining the stress state of a structure under typical loading conditions. The lines originating from P=Q=0 depicted on this plot demarcate specific loading conditions.

Figure 2. Discs set in dental cement and ready for sectioning into test specimens using a precision anular saw.

Figure 3. Schematic representations of an IVD and anulus fibrosus sample showing (A). An isolated IVD, with posterior elements removed, showing the three regions of disc from which samples were obtained and the cutting planes used to create square cross-section samples shown in greyscale; (B). A single anulus fibrosus sample, demonstrating that for a sample cross- sectional dimension of 3mm x 3mm there were no collagen fibres linking adjacent vertebral/cartilage endplates; (C). Collagen fibre inclination in each sample.

Figure 4. Biaxial compression device. (A) Assembled, (B) View inside vessel showing viewing windows and specimen connected to the moving piston and rigid attachment (NB. For the purpose of illustration, there is no fluid in the vessel), and (C) Details of the ceramic piston to which the specimen is attached.

Figure 5. Schematic of experimental set-up for simple shear testing on a Hounsfield testing machine.

Figure 6. Uniaxial compression response. (LoBF = line of best fit) (A) Typical experimental response, (B) Highly reproducible response, (C) Schematic representations demonstrating the separation of adjacent lamellae during compressive testing of an anulus fibrosus specimen. Note that these interlaminar separations do not necessarily occur centrally within the specimen, in the radial direction, (D) Regression LoBF.

Figure 7. Simple shear response. (A) Typical experimental response and (B) Regression LoBF.

Figure 8. Biaxial compression response. (A) Measured circumferentially, showing an obvious drop in stiffness between Cycle 1 and the remaining tests. (B) Measured radially, showing no difference in response between the initial and repeated loading, (C) Measured radially, showing a drop in stiffness between Cycle 1 and the remaining tests, but mainly at low strains, (D) and (E) Regression LoBF for circumferential and radial measurements, respectively. (Note: the anterior initial and continued responses were the same when measured radially, as shown in (E)).

.

7. REFERENCES

Acaroglu, E. R., Iatridis, J. C., Setton, L. A., Foster, R. J., Mow, V. C.,Weidenbaum, M., 1995. Degeneration and aging affect the tensile behaviour of human lumbar annulus fibrosus. Spine 20(24): 2690-2701.

Adams, M. A.,Green, T. P., 1993. Tensile properties of the anulus fibrosus i. The contribution of fibre-matrix interactions to tensile stiffness and strength. Eur Spine J 2: 203-208.

Adams, M. A., Hutton, W. C.,Stott, J. R., 1980. The resistance to flexion of the lumbar intervertebral joint. Spine 5(3): 245-53.

Akeson, W. H., Woo, S. L., Taylor, T. K., Ghosh, P.,Bushell, G. R., 1977. Biomechanics and biochemistry of the intervertebral disks: The need for correlation studies. Clin Orthop Relat Res(129): 133-40.

Bass, E. C., Ashford, F. A., Segal, M. R.,Lotz, J. C., 2004. Biaxial testing of human annulus fibrosus and its implications for a constitutive formulation. Ann Biomed Eng 32(9): 1231-42.

Bass, E. C., Duncan, N. A., Hariharan, J. S., Dusick, J., Bueff, H. U.,Lotz, J. C., 1997. Frozen storage affects the compressive creep behavior of the porcine intervertebral disc. Spine (Phila Pa 1976) 22(24): 2867-76.

Best, B. A., Guilack, F., Setton, L. A., Zhu, W., Saed-Nejad, F., Ratcliffe, A., Weidenbaum, M.,Mow, V., 1994. Compressive mechanical properties of the human anulus fibrosus and their relationship to biochemical composition. Spine 19(2): 212-221.

Callaghan, J. P.,McGill, S. M., 1995. Frozen storage increases the ultimate compressive load of porcine vertebrae. J Orthop Res 13(5): 809-12.

Ebara, S., Iatridis, J. C., Setton, L. A., Foster, R. J., Mow, V. C.,Weidenbaum, M., 1996. Tensile properties of nondegenerate human lumbar annulus fibrosus. Spine 21(4): 452-461.

Fujita, Y., Duncan, N. A.,Lotz, J. C., 1997. Radial tensile properties of the lumbar annulus fibrosus are site and degeneration dependent. Journal of Orthopaedic Research 15: 814-9.

Fujita, Y., Wagner, D. R., Biviji, A. A., Duncan, N. A.,Lotz, J. C., 2000. Anisotropic shear behaviour of the annulus fibrosus: Effect of harvest site and tissue prestrain. Medical Engineering and Physics 22: 349-57.

Higginson, G. R., Litchfield, M. R.,Snaith, J., 1976. Load-displacement characteristics of articular cartilage. International Journal of Mechanical Sciences 18(9-10): 481-86.

Iatridis, J. C., Kumar, S., Foster, R. J., Weidenbaum, M.,Mow, V. C., 1999. Shear mechanical properties of human lumbar annulus fibrosus. Journal of Orthopaedic Research 17: 732-37.

Iatridis, J. C., MaClean, J. J.,Ryan, D. A., 2005. Mechanical damage to the intervertebral disc annulus fibrosus subjected to tensile loading. J Biomech 38(3): 557-65.

Iatridis, J. C., Setton, L. A., Foster, R. J., Rawlins, B. A., Weidenbaum, M.,Mow, V. C., 1998. Degeneration affects the anisotropic and nonlinear behaviors of human anulus fibrosus in compression. Journal of Biomechanics 31: 535-44.

Kasra, M., Parnianpour, M., Shirazi-Adl, A., Wang, J. L.,Grynpas, M. D., 2004. Effect of strain rate on tensile properties of sheep disc anulus fibrosus. Technol Health Care 12(4): 333-42.

Kasra, M., Shirazi-Adl, A.,Drouin, G., 1992. Dynamics of human lumbar intervertebral joints. Experimental and finite-element investigations. Spine 17(1): 93-102.

Klein, J. A.,Hukins, D. W. L., 1983. Functional differentiation in the spinal column. Engineering in Medicine 12(2): 83-85.

Lieu, C., Nguyen, T.,Payant, L., 2001. In vitro comparison of peak polymerisation temperatures of 5 provisional restoration resins. Journal of Canadian Dental Association 67(1): 36-39.

Little, J. P. (2004). Finite element modelling of anular lesions in the lumbar intervertebral disc. School of Mechanical, Manufacturing and Medical Engineering Queensland University of Technology. Brisbane, Australia. **Doctor of Philosophy**. http://adt.library.qut.edu.au./adt-qut/public/adt-QUT20050517.141125

Little, J. P., Adam, C., Evans, J. H., Pettet, G. J.,Pearcy, M. J., 2007. Nonlinear finite element analysis of anular lesions in the l4/5 intervertebral disc. Journal of Biomechanics 40(12): 2744-2751.

Little, J. P., Tevelen, G., Adam, C. J., Evans, J. H.,Pearcy, M. J., 2009. Development of a biaxial compression device for biological samples: Preliminary experimental results for a closed cell foam. Journal of Mechanical Behavior of Biomedical Materials 2(3): 305-9.

Marchand, F.,Ahmed, A. M., 1990. Investigation of the laminate structure of lumbar disc anulus fibrosus. Spine 15(5): 402-10.

Morgan, F. R., 1960. The mechanical properties of collagen fibres: Stress-strain curves. Journal of the Society of Leather Trades' Chemists. 44: 170-.

Nachemson, A., 1960. Lumbar intradiscal pressure: Experimental studies on post-mortem material. Acta Orthopaedica Scandinavica 43.

Panjabi, M. M., Krag, M., Summers, D.,Videman, T., 1985. Biomechanical time-tolerance of fresh cadaveric human spine specimens. J Orthop Res 3(3): 292-300.

Pezowicz, C. A., Robertson, P. A.,Broom, N. D., 2006. The structural basis of interlamellar cohesion in the intervertebral disc wall. J Anat 208(3): 317-30.

Reid, J. E., Meakin, J. R., Robins, S. P., Skakle, J. M.,Hukins, D. W., 2002. Sheep lumbar intervertebral discs as models for human discs. Clinical Biomechanics (Bristol, Avon) 17(4): 312-4.

Rohlmann, A., Zander, T., Schmidt, H., Wilke, H.-J.,Bergmann, G., 2006. Analysis of the influence of disc degeneration on the mechanical behaviour of a lumbar motion segment using the finite element method. Journal of Biomechanics 39: 2484-2490.

Schollum, M. L., Robertson, P. A.,Broom, N. D., 2008. Issls prize winner: Microstructure and mechanical disruption of the lumbar disc annulus: Part i: A microscopic investigation of the translamellar bridging network. Spine (Phila Pa 1976) 33(25): 2702-10.

Shirazi-Adl, A., Ahmed, A. M.,Shrivastava, S. C., 1986. Mechanical response of a lumbar motion segment in axial torque alone and combined with compression. Spine 11(9): 914-27.

Skaggs, D. L., Weidenbaum, M., Iatridis, J. C., Ratcliffe, A.,Mow, V. C., 1994a. Regional variation in tensile properties and biochemical composition of the human lumbar anulus fibrosus. Spine 19(12): 1310-1319.

Skaggs, D. L., Weidenbaum, M., Iatridis, J. C., Ratcliffe, A.,Mow, V. C., 1994b. Regional variation in tensile properties and biochemical composition of the human lumbar anulus fibrosus. Spine 19(12): 1310-9.

Smith, L. J., Byers, S., Costi, J. J.,Fazzalari, N. L., 2008. Elastic fibers enhance the mechanical integrity of the human lumbar anulus fibrosus in the radial direction. Ann Biomed Eng 36(2): 214-23.

Thompson, R. E., Barker, T., M.,,Pearcy, M. J., 2003. Defining the neutral zone of sheep intervertebral joints during dynamic motions: An in vitro study. Clinical Biomechanics 18: 89-98.

Treloar, L. R. G., 1975. The physics of rubber elasticity, 3rd. Oxford University Press, London.

Wagner, D. R.,Lotz, J. C., 2004. Theoretical model and experimental results for the nonlinear elastic behavior of human annulus fibrosus. J Orthop Res 22(4): 901-9.

Wilke, H., Kettler, A.,Claes, L., 1997. Are sheep spines a valid biomechanical model for human spines? Spine 22(20): 2365-2374.

Wu, H.,Yao, R., 1976. Mechanical behavior of the human annulus fibrosus. Journal of Biomechanics 9: 1-7.

Yu, J., Winlove, P. C., Roberts, S.,Urban, J. P., 2002. Elastic fibre organization in the intervertebral discs of the bovine tail. J Anat 201(6): 465-75.

Zander T, Rohlmann A, Calisse J, Bergmann G. 2001 Estimation of muscle forces in the lumbar spine during upper-body inclination. Clinical Biomechanics 16(Suppl 1): S73-80.

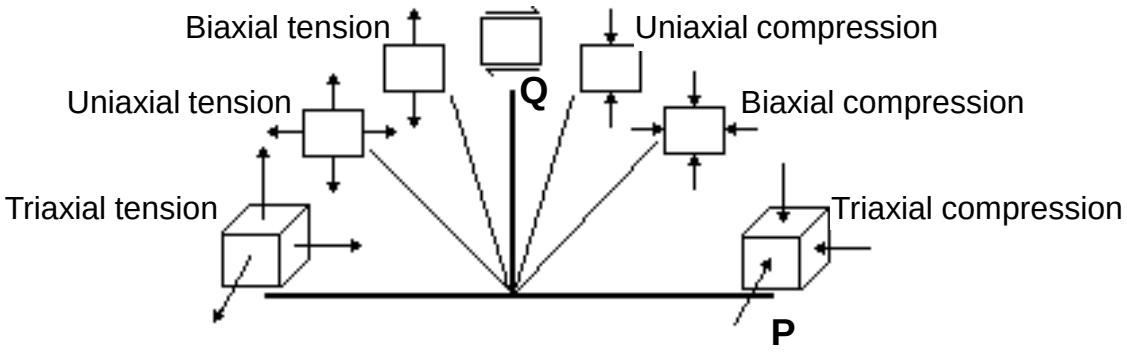

Figure 1

Caption: P-Q curve defining the stress state of a structure under typical loading conditions. The lines originating from P=Q=0 depicted on this plot, demarcate specific loading conditions.

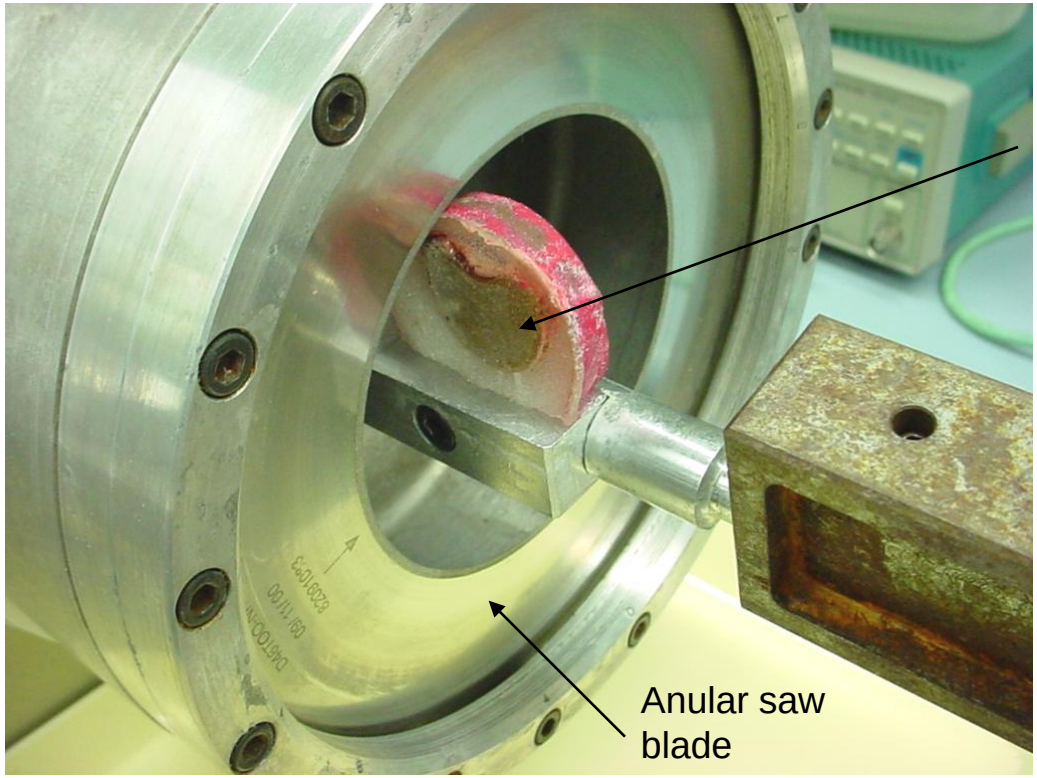

Caption: Discs set in dental cement and ready for sectioning into test specimens using a precision anular saw.

Figure 2

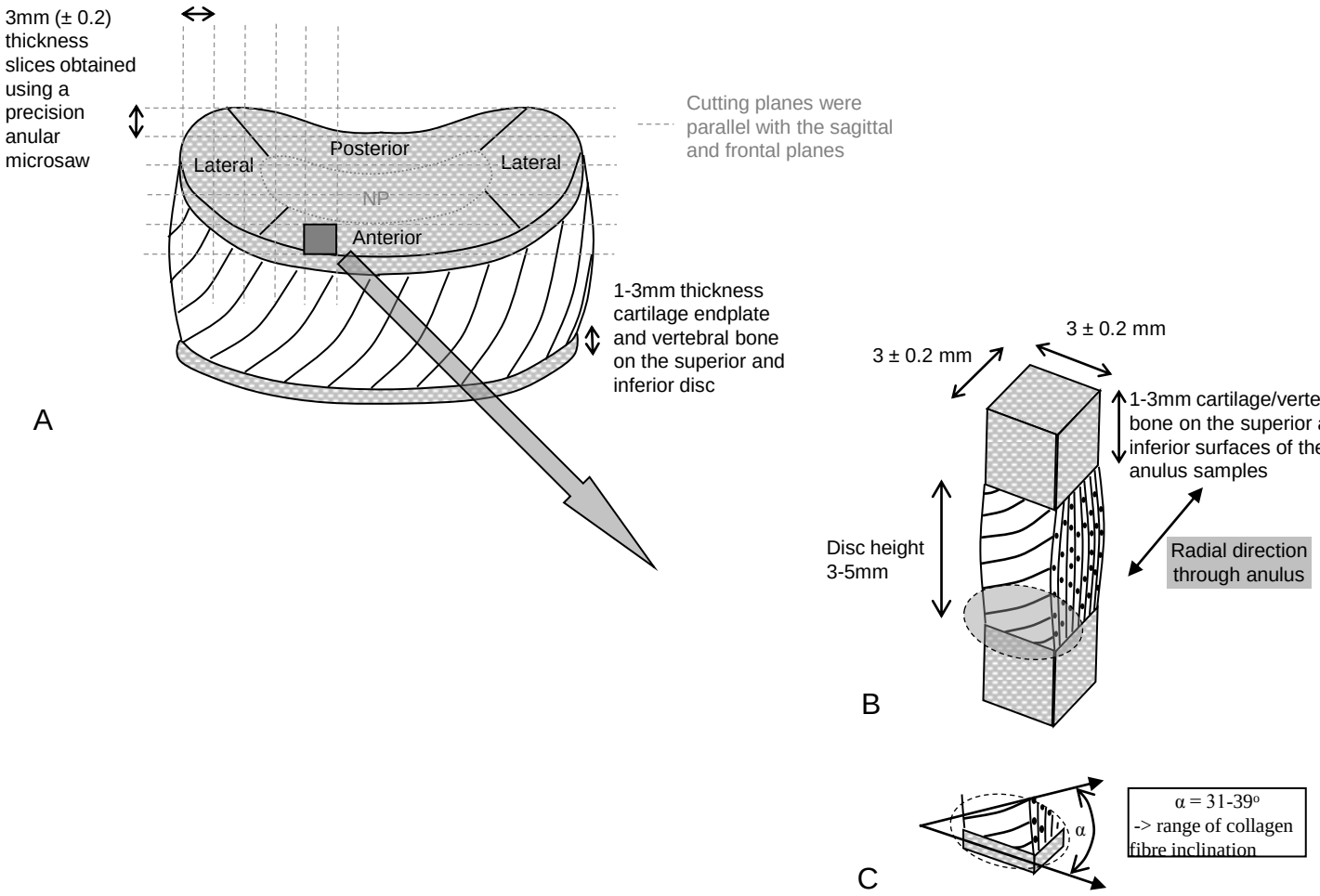

Figure 3

Caption: Schematic representations of an intervertebral disc and anulus fibrosus sample showing A. An isolated intervertebral disc, with posterior elements removed, showing the three regions of disc from which samples were obtained and the cutting planes used to create square cross-section samples shown in greyscale; B. A single anulus fibrosus sample, demonstrating that for a sample cross sectional dimension of 3mm x 3mm there were no collagen fibres linking adjacent vertebral/cartilage endplates; C. Collagen fibre inclination in each sample.

A

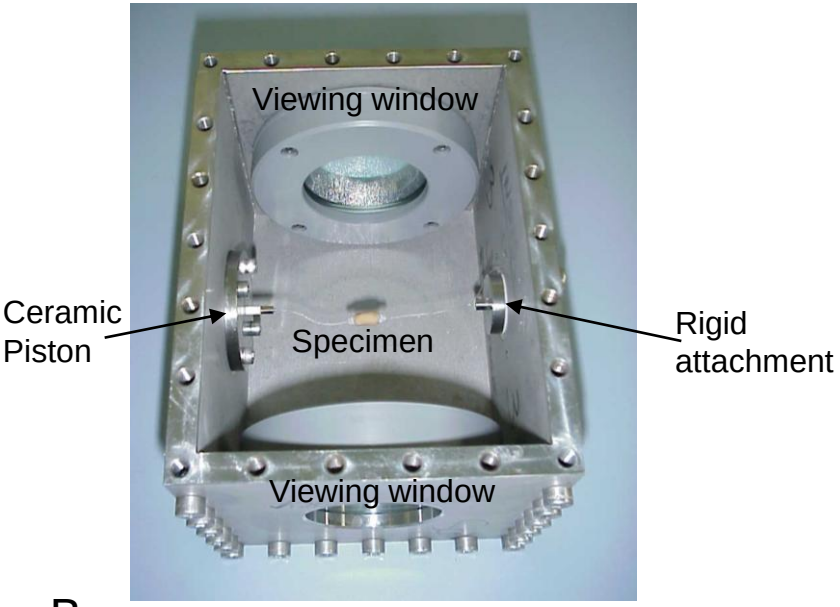

B

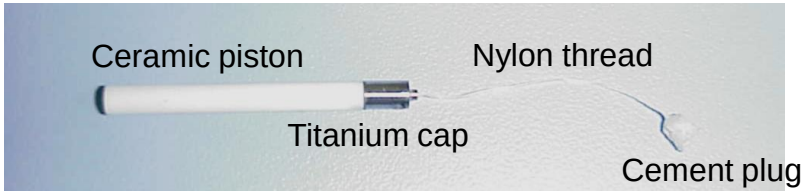

C

Figure 4

Caption: A. Biaxial Compression device. A. Assembled, B. View inside vessel showing viewing windows and specimen connected to the moving piston and rigid attachment (NB. For the purpose of illustration, there is no fluid in the vessel), C. Details of the ceramic piston to which specimen is attached.

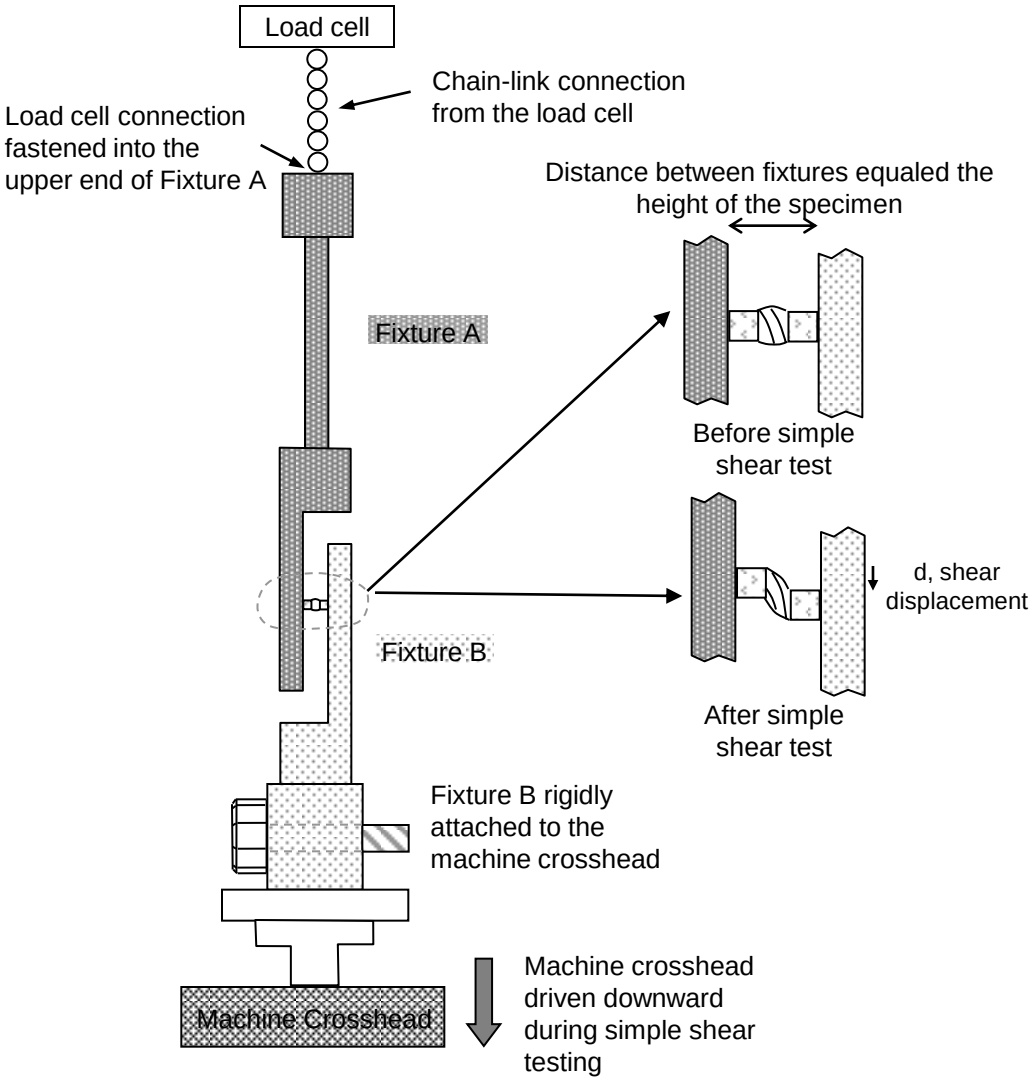

Figure 5

Caption: Schematic of experimental set-up for simple shear testing on a Hounsfield testing machine.

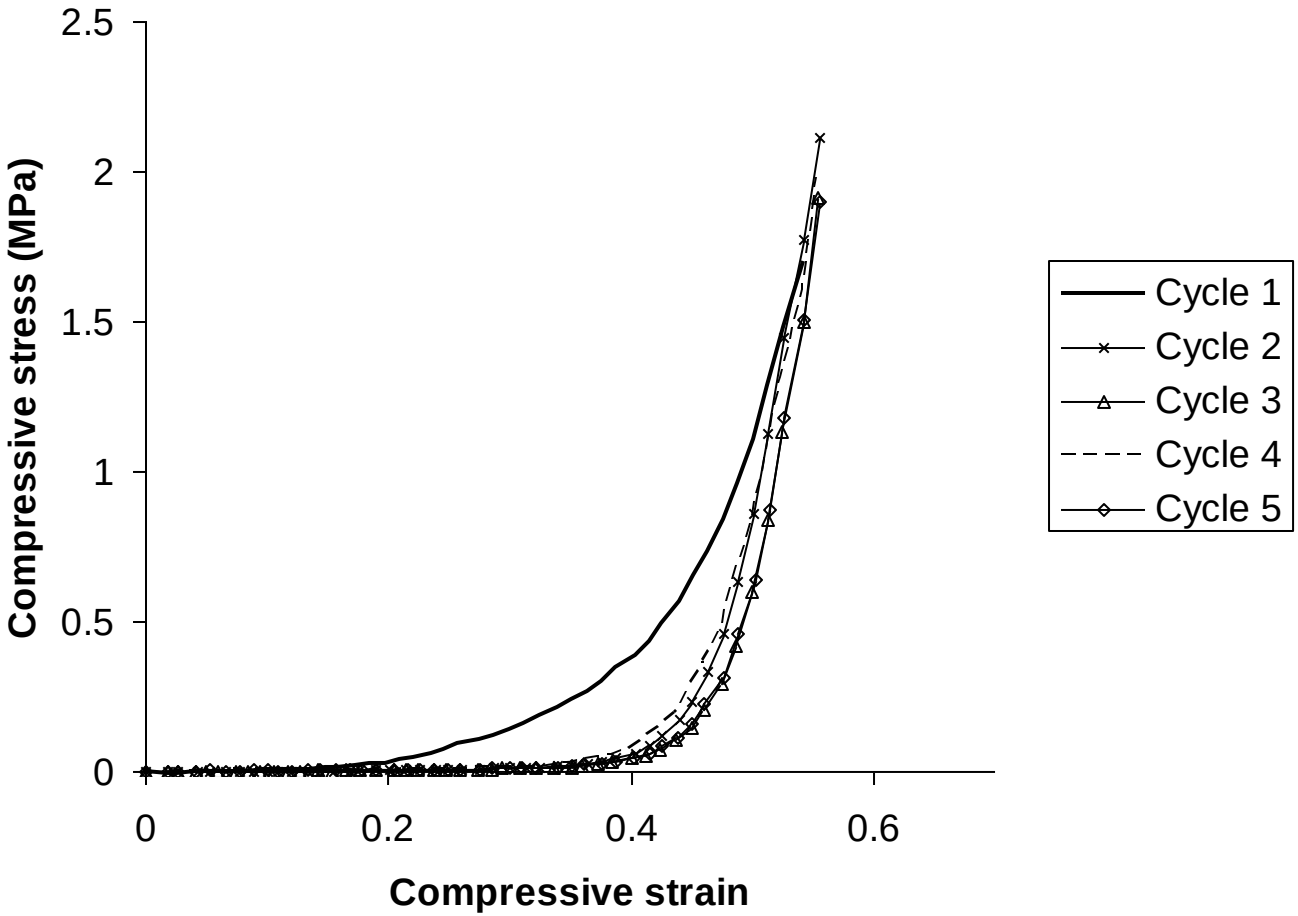
2.5
2
1.5
1
0.5
0
Compressive stress (MPa)
0
0.2
0.4
0.6
Compressive strain
Cycle 1
Cycle 2
Cycle 3
Cycle 4
Cycle 5

Figure 6 A

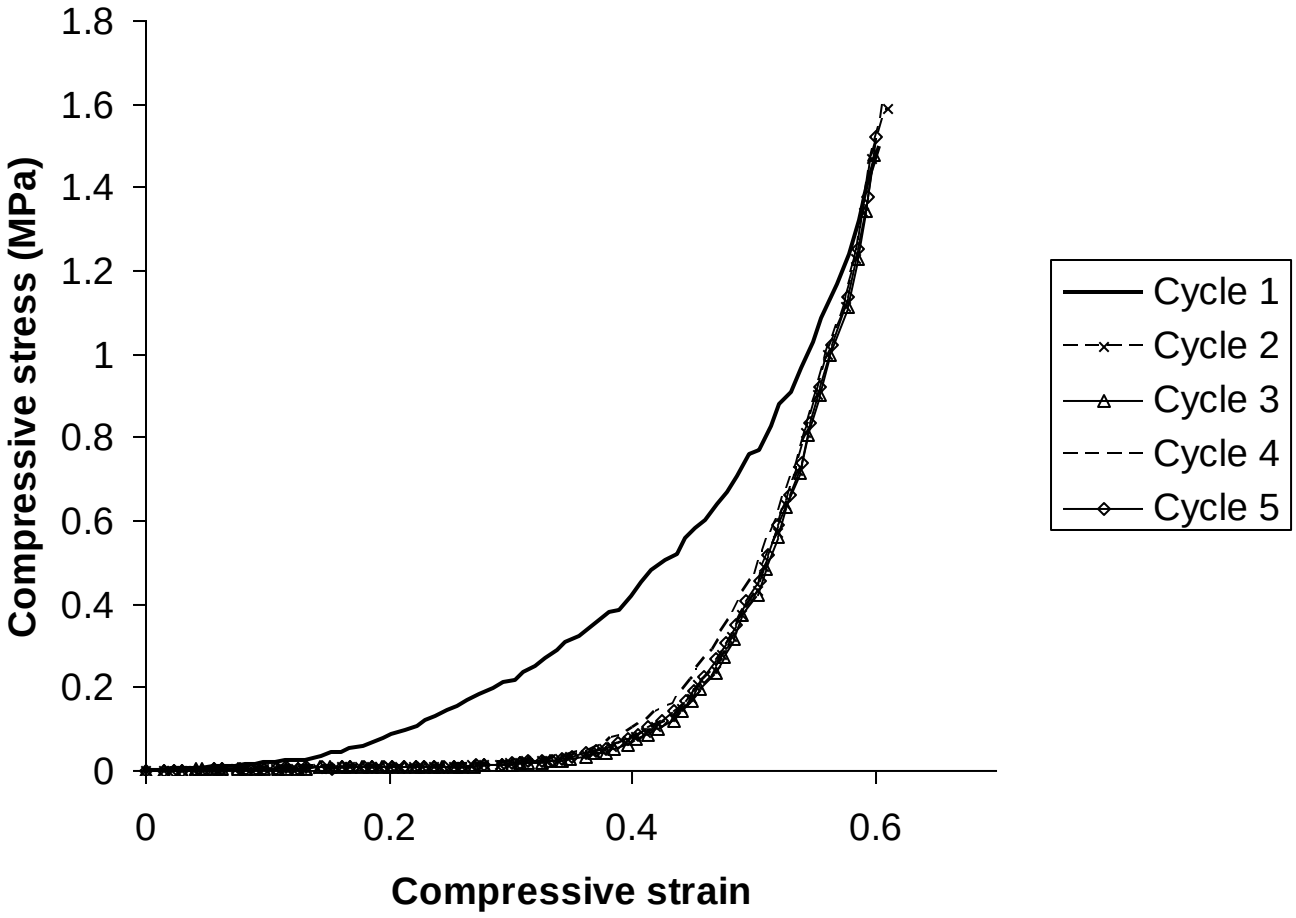
1.8
1.6
1.4
1.2
1
0.8
0.6
0.4
0.2
0
Compressive stress (MPa)
0
0.2
0.4
0.6
Compressive strain
Cycle 1
Cycle 2
Cycle 3
Cycle 4
Cycle 5

Figure 6 B

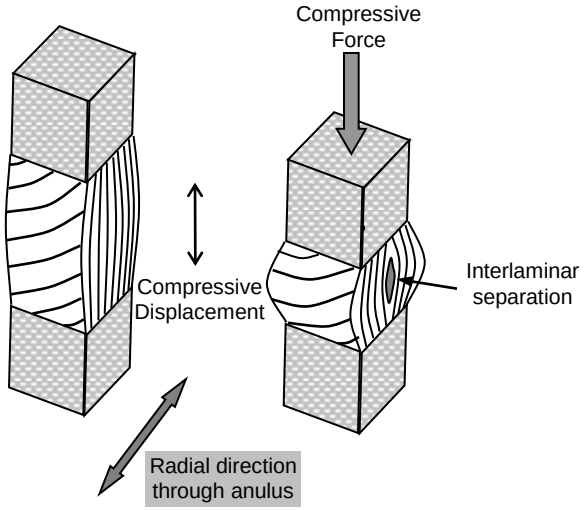
Compressive
Force
Compressive
Displacement
Interlaminar
separation
Radial direction
through anulus

Figure 6 C

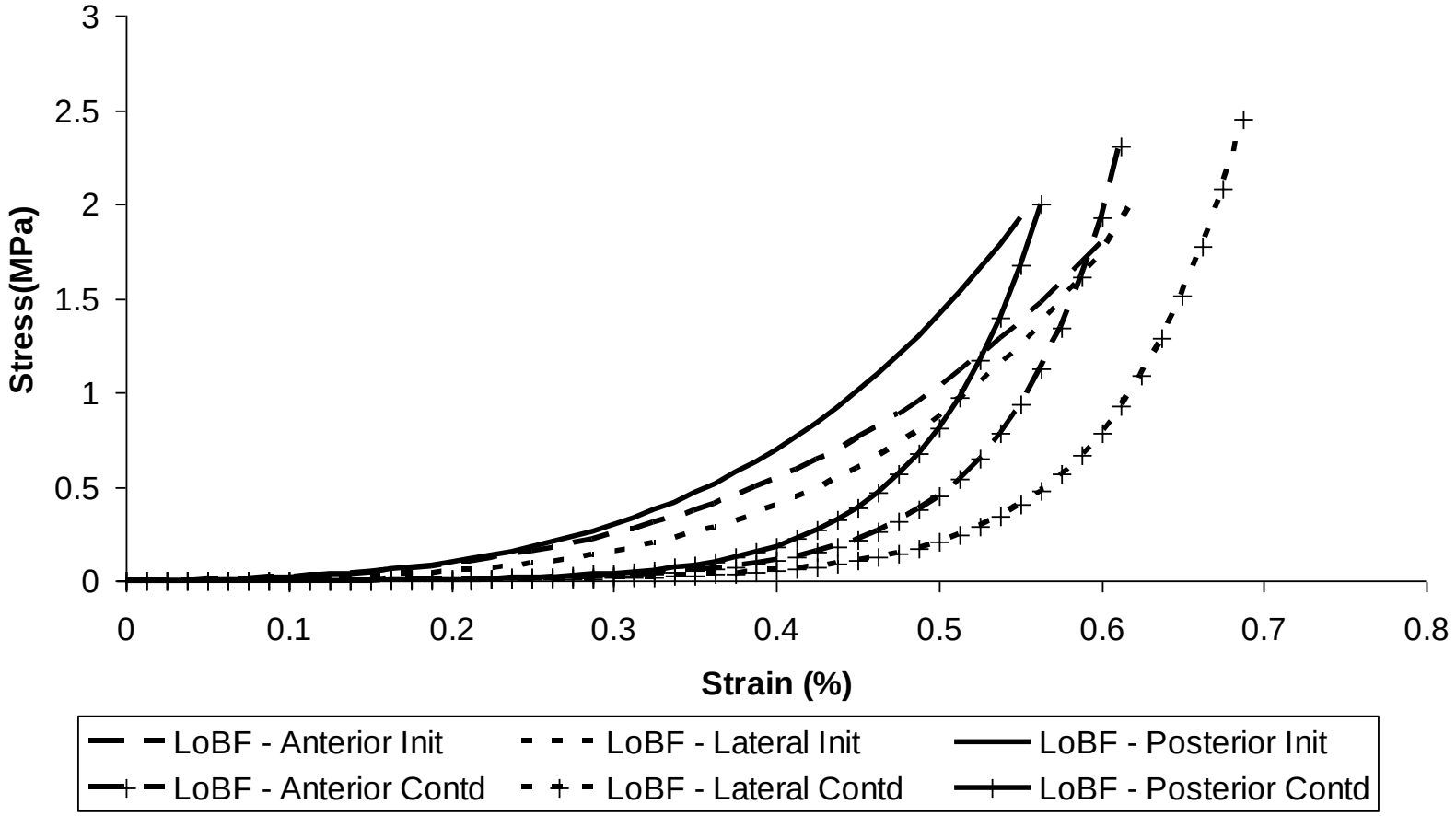

Caption: Uniaxial compression response. (LoBF=Line of best fit) A. Typical experimental response, B. Highly reproducible response, C. Schematic representations demonstrating separation of adjacent lamellae during compressive testing of an anulus fibrosus specimen. Note that these interlaminar separations do not necessarily occur centrally within the specimen, in the radial direction. D. Regression lines-of-best fit

Figure 6 D

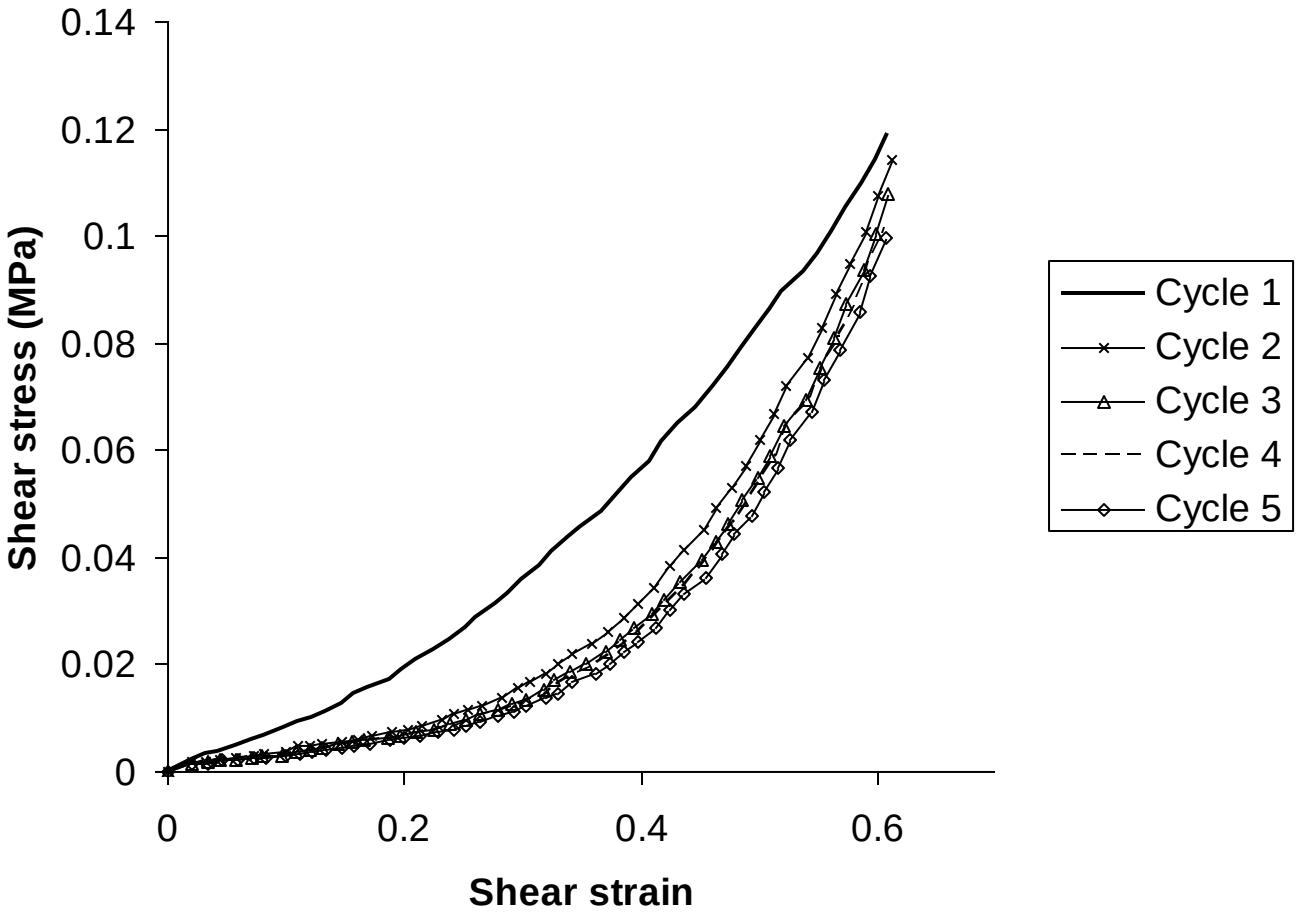
0.14
0.12
0.1
0.08
0.06
0.04
0.02
0
Shear stress (MPa)
0
0.2
0.4
0.6
Shear strain
Cycle 1
Cycle 2
Cycle 3
Cycle 4
Cycle 5

Figure 7 A

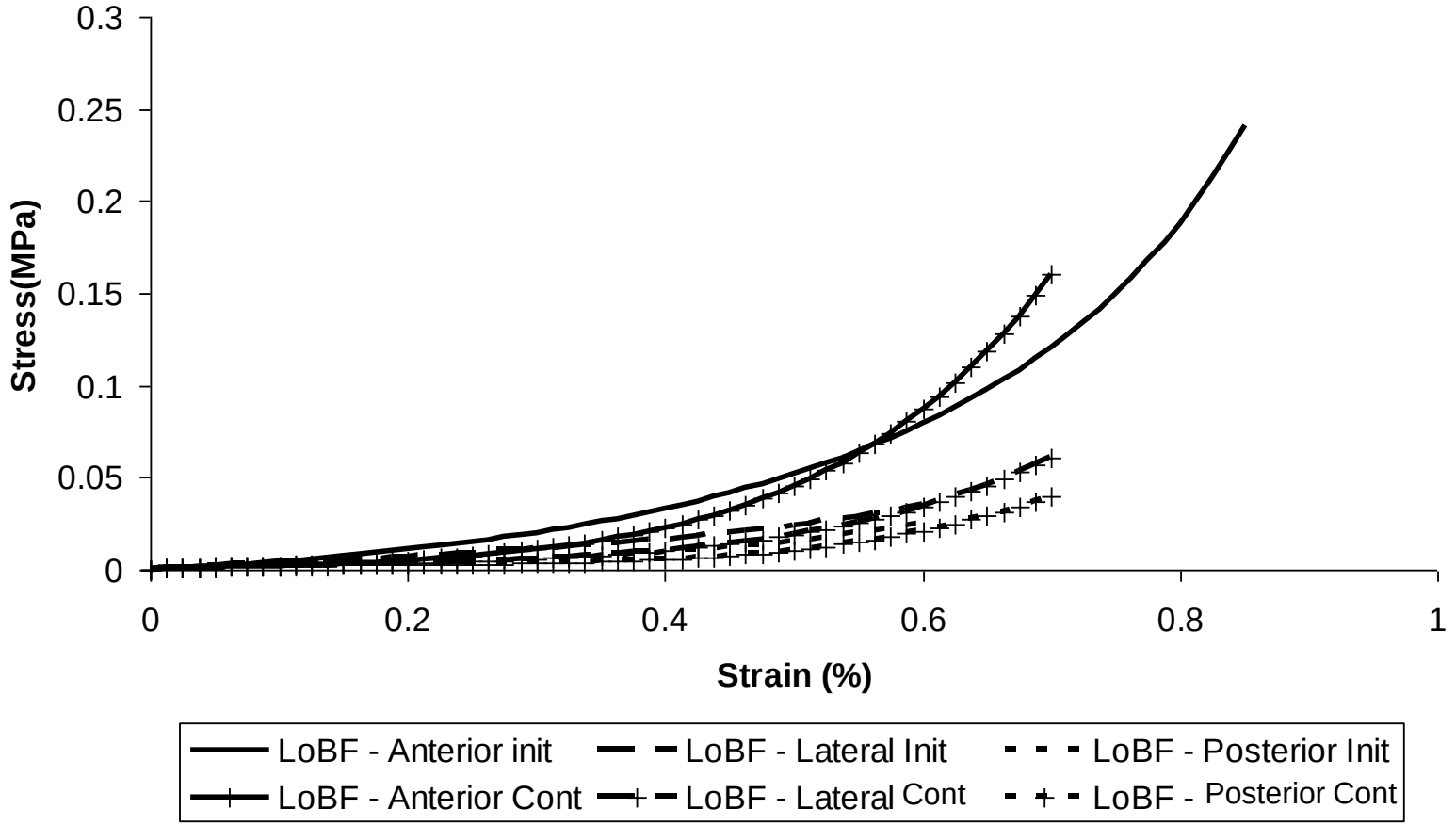

Caption: Simple shear response. A. Typical experimental response, B. Regression lines-of-best fit

Figure 7 B

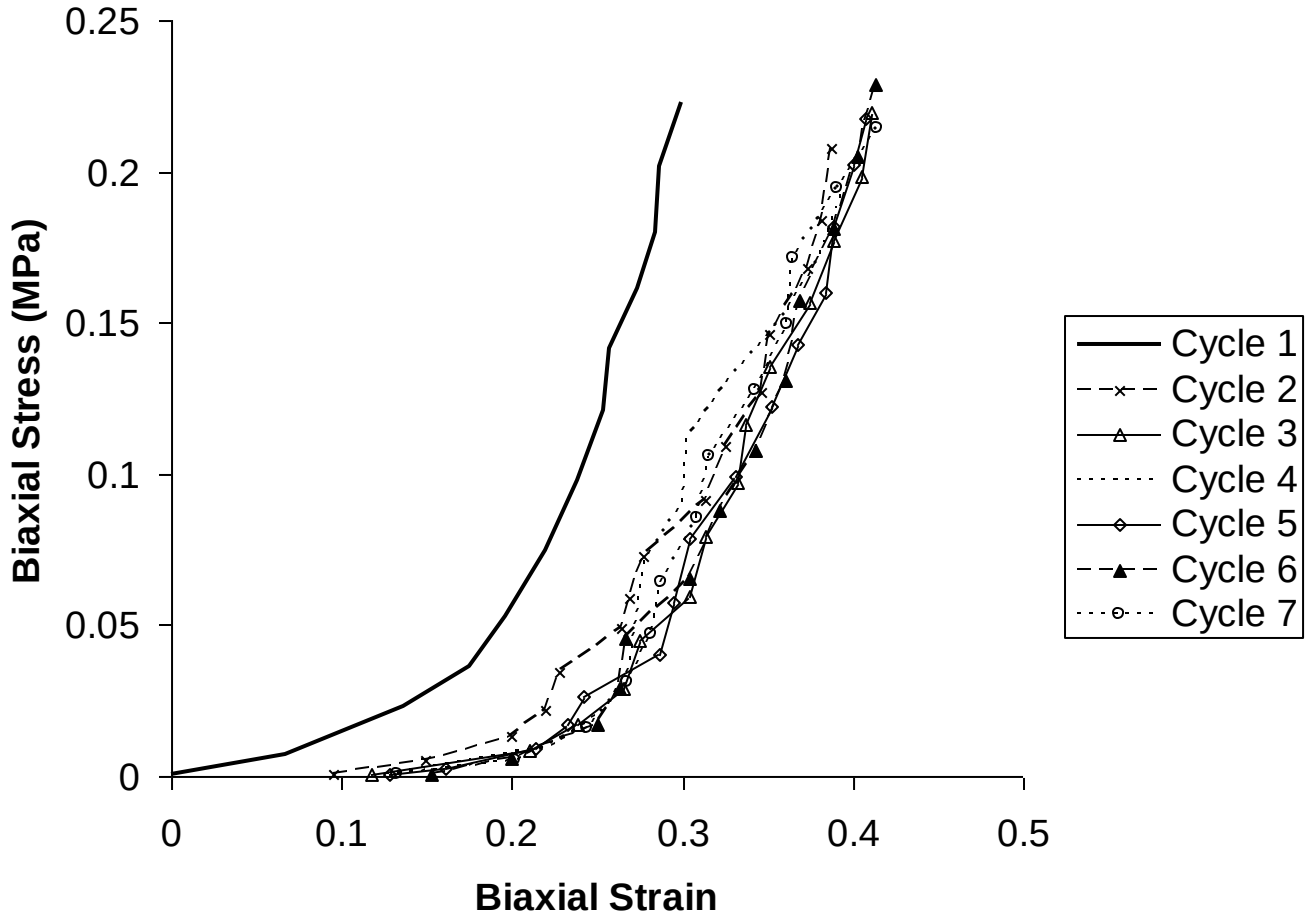
0.25
0.2
0.15
0.1
0.05
0
Biaxial Stress (MPa)
0
0.1
0.2
0.3
0.4
0.5
Biaxial Strain
Cycle 1
Cycle 2
Cycle 3
Cycle 4
Cycle 5
Cycle 6
Cycle 7

Figure 8 A

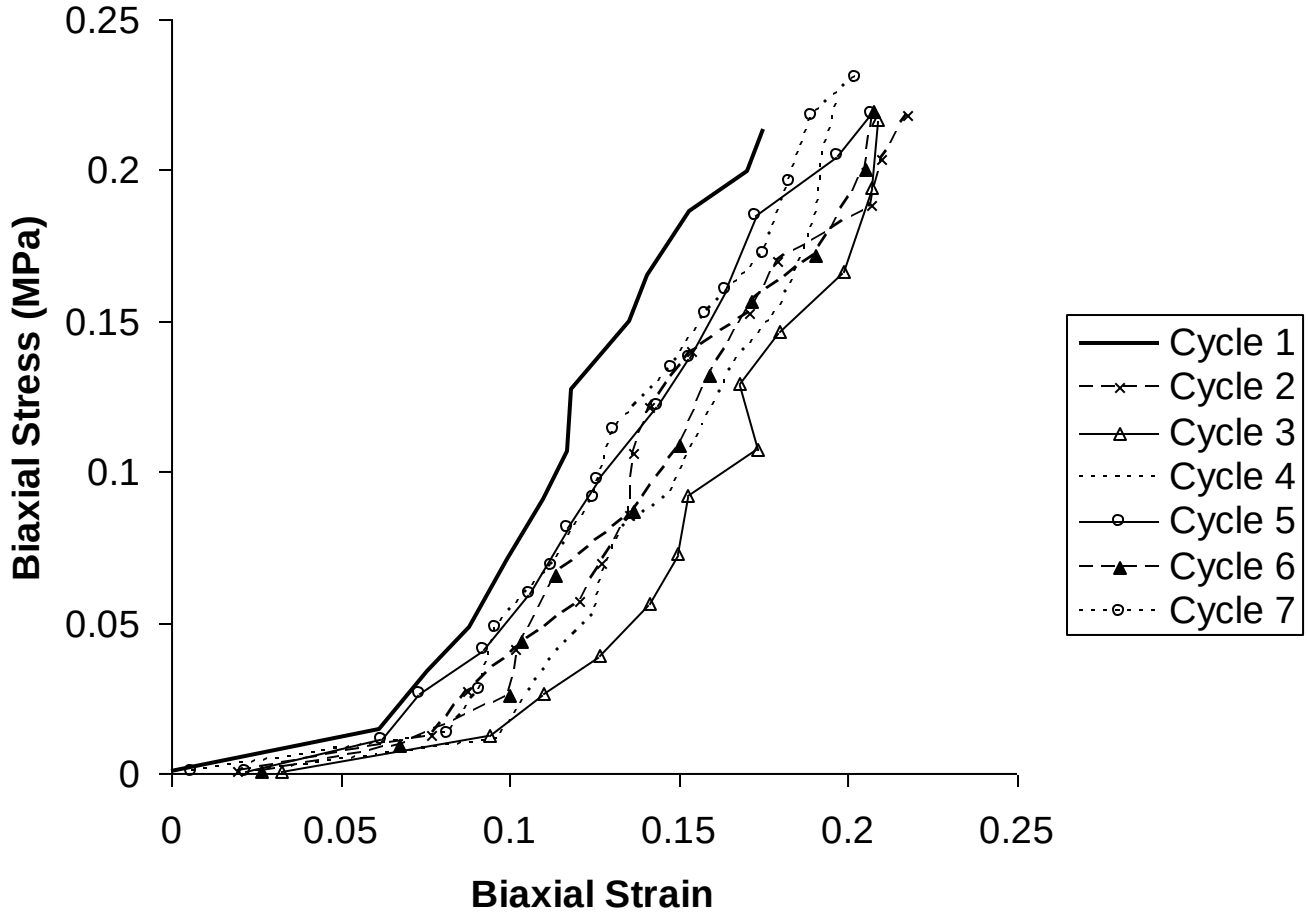
0.25
0.2
0.15
0.1
0.05
0
Biaxial Stress (MPa)
0
0.05
0.1
0.15
0.2
0.25
Biaxial Strain
Cycle 1
Cycle 2
Cycle 3
Cycle 4
Cycle 5
Cycle 6
Cycle 7

Figure 8 B

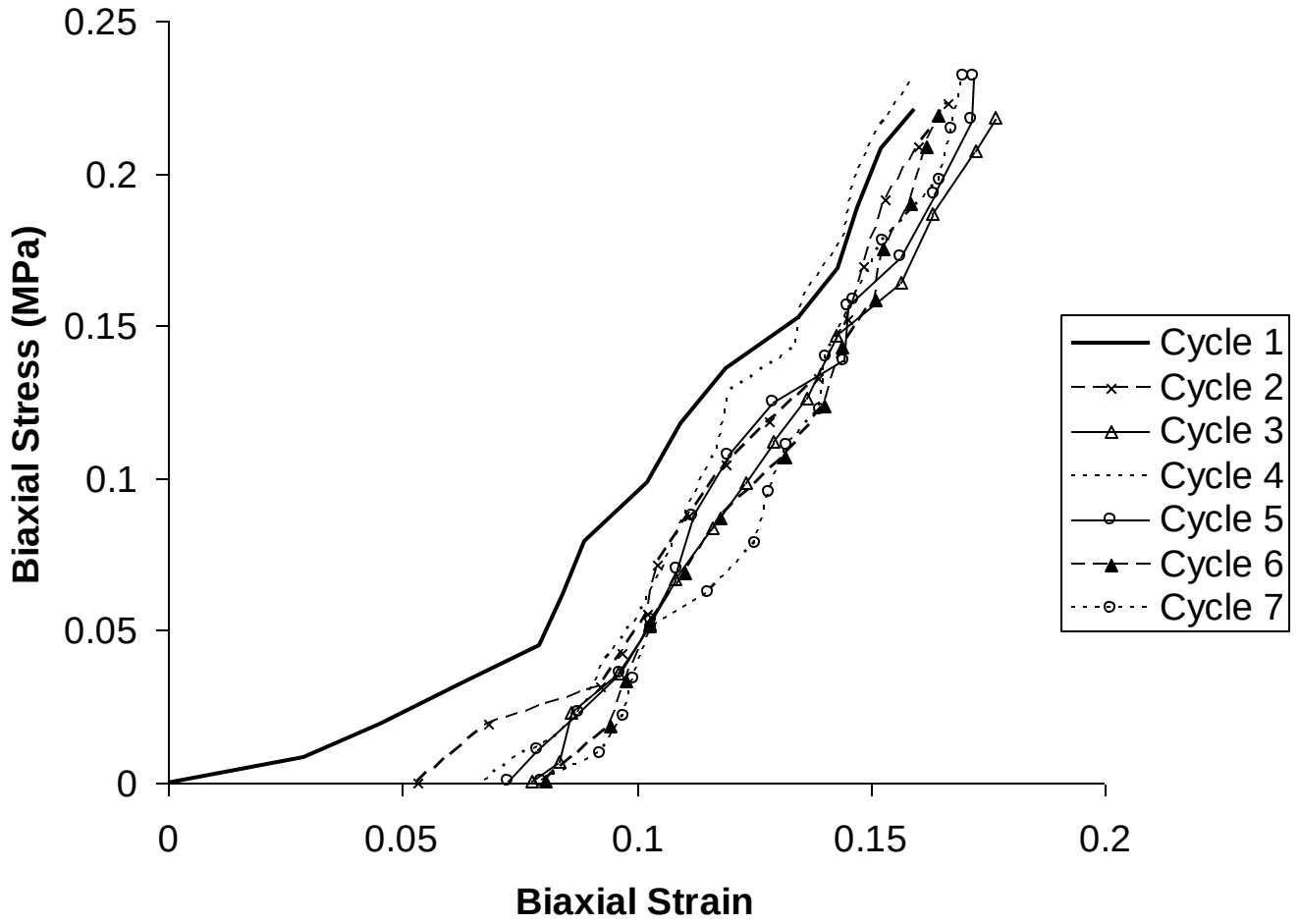
0.25
0.2
0.15
0.1
0.05
0
Biaxial Stress (MPa)
0
0.05
0.1
0.15
0.2
Biaxial Strain
Cycle 1
Cycle 2
Cycle 3
Cycle 4
Cycle 5
Cycle 6
Cycle 7

Figure 8 C

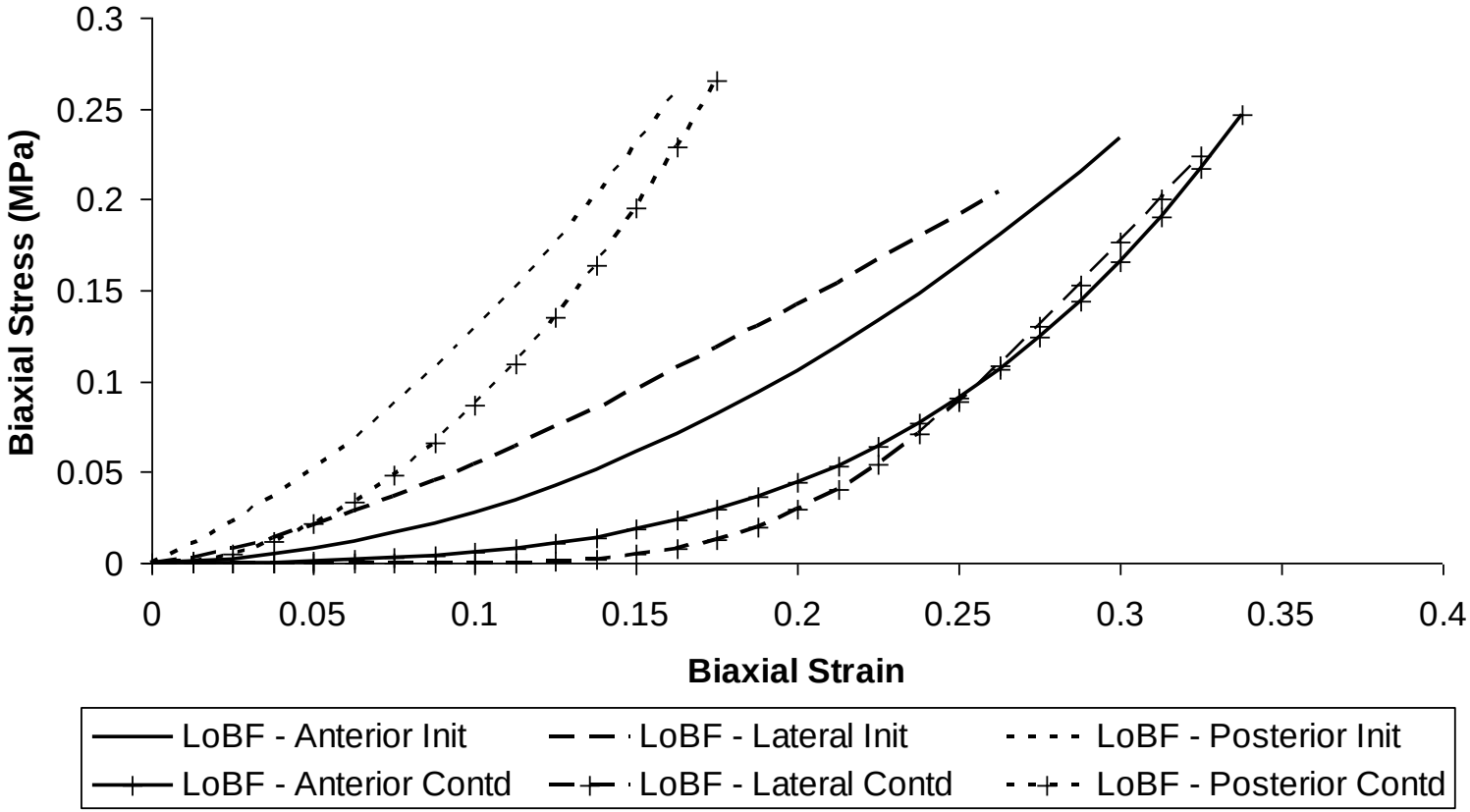
0.3
0.25
0.2
0.15
0.1
0.05
0
Biaxial Stress (MPa)
0
0.05
0.1
0.15
0.2
0.25
0.3
0.35
0.4
Biaxial Strain
LoBF - Anterior Init
LoBF - Lateral Init
LoBF - Posterior Init
LoBF - Anterior Contd
LoBF - Lateral Contd
LoBF - Posterior Contd

Figure 8 D

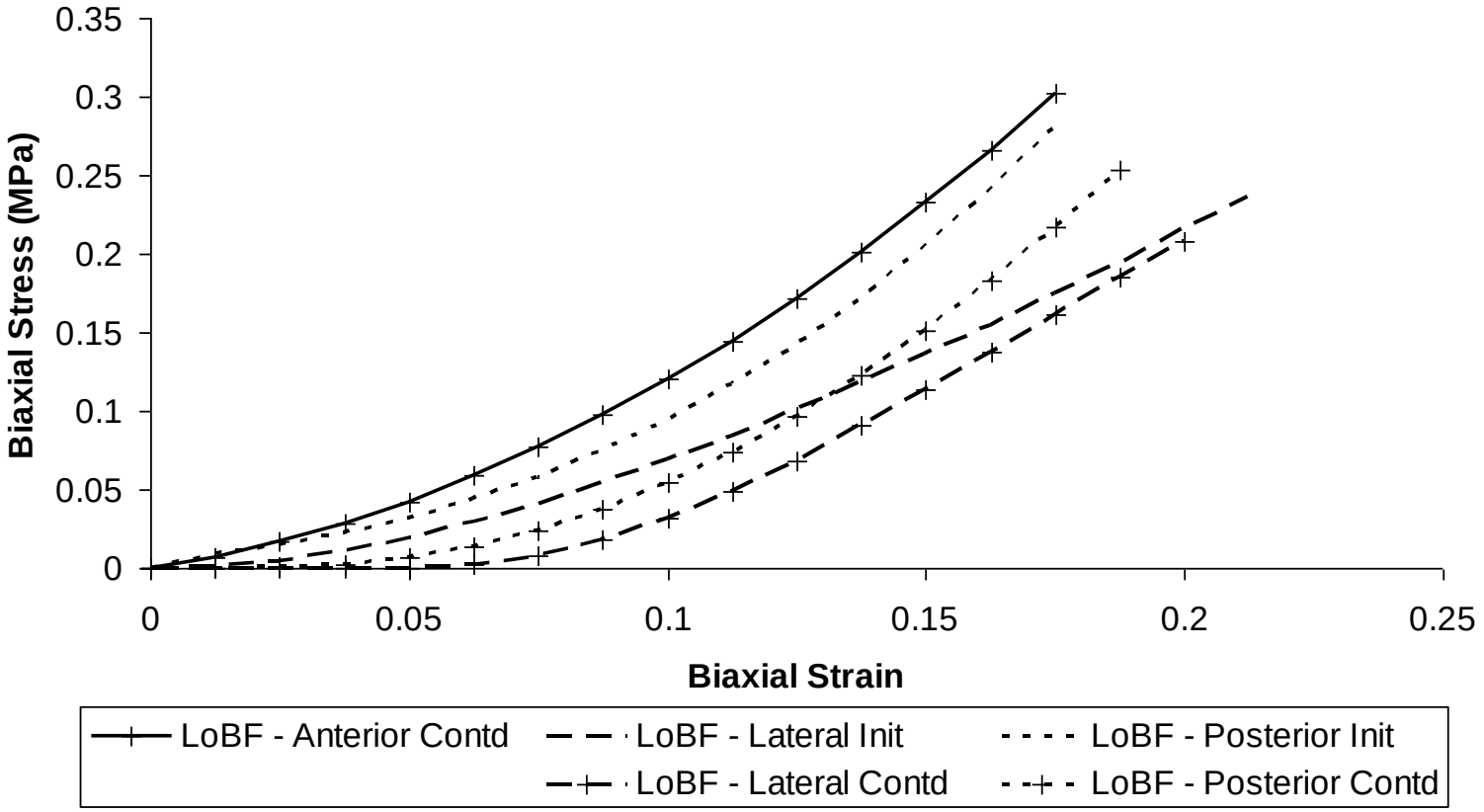

Figure 8 E

Caption: A. Biaxial compression response measured circumferentially, showing an obvious drop in stiffness between Cycle 1 and the remaining tests; B. Response measured radially, showing no difference in response between the initial and repeating loading; C. Response measured radially, showing a drop in stiffness between Cycle 1 and the remaining tests, but mainly at low strains. D, E. Regression lines-of-best fit for circumferential and radial measurement, respectively. (Note: The anterior initial and continued responses were the same when measured radially, as shown in E.)